Three-body calculation of ^{9}Be electromagnetic observables

E. Cravo
Centro de Física Nuclear, Universidade de Lisboa, Av. Prof. Gama Pinto 2, P-1699 Lisboa, Portugal
(Received 27 March 1996)

A three-body calculation of the electromagnetic observables of the ^{9}Be ground state is reported. The nucleus of ^{9}Be is considered as a three-body system of one neutral plus two charged particles: $n+\alpha+\alpha$. Simple two-body n-α and α-α potentials, plus Coulomb, constitute the only input to the momentum-space three-body equations. No adjustable parameters are used. The equations are solved numerically for the ground state, generating simultaneously the binding energy and wave function. The normalized wave function is then used in the calculation of the matrix elements of the electromagnetic operators. The neutron and alpha particle form factors are folded in this calculation. Results are presented for ^{9}Be elastic longitudinal and transverse form factors, and static multipole moments: rms charge radius, electric quadrupole moment, and magnetic dipole and octupole moments. [S0556-2813(96)02808-7]

PACS number(s): 21.45.+v, 21.60.Gx, 21.10.Ky

I. INTRODUCTION

The ^{9}Be nucleus presents a low neutron separation energy. Its low-energy excited states are unstable and break up into one of the forms, $\alpha+{}^5$He or $n+{}^8$Be, where both ^{5}He and ^{8}Be are unbound nuclei decaying to $\alpha+n$ and $\alpha+\alpha$, respectively. All other forms of breakup require excitation energies above 16 MeV. These facts suggest a high degree of clustering of the ^{9}Be nucleus. The nucleons appear to be organized as a weak bound state of three clusters consisting of two alpha particles plus one odd neutron. The four nucleons in the alpha particle are so strongly bound in proportion to the neutron separation energy in ^{9}Be that, for low excitation energies, one may consider the alpha particle as elementary. This assumption sets the ground for a three-body model calculation of ^{9}Be, where the neutron and the two alpha particles interact through effective potentials.

So far the models used in theoretical descriptions of this nucleus have been based essentially on effective one- and two-body dynamical equations—shell model, Nilsson model, projected Hartree-Fock, cluster model RGM (see references in [1–3]); approximate three-body models—Born-Oppenheimer three-body molecular model [4]; and more recently a variational three-body calculation based on a Gaussian ansatz [5]. In this respect, the present work constitutes an attempt to represent the ^{9}Be nuclear ground state as a three-body system where the dynamics is determined by exact three-body equations [6].

The equations derived for the bound state of the $n+\alpha+\alpha$ system are a generalization of the ones presented by Lehman *et al.* [7] for the case of spinless, one neutral plus two charged, particles with identical mass. Here the fermionic character of the neutron together with its different mass is taken into account. After separation of the center-of-mass motion and partial wave expansion, a set of coupled momentum-space integral equations in two continuous variables is obtained. This set of coupled equations is solved numerically for the ground state, using the method of inverse iteration, producing simultaneously the binding energy and the wave function components.

Both ground-state energy and three-body wave function are completely determined from the solution of the bound-state equations. They are exclusively dependent on the two-body interactions used, and contain no adjustable parameters. The wave function thus obtained is, after normalization, used in the calculation of the elastic electromagnetic form factors. For this purpose, the finite size and nonelementary character of the alpha particle and the neutron are taken into account through the use of phenomenological electric and magnetic form factors for these particles. Finally the ground-state electromagnetic moments of ^{9}Be are evaluated by taking the static limit of the corresponding multipole terms.

Section II contains a brief survey of the two-body n-α and α-α potentials used in the present calculations. The derivation of the three-body equations and the results obtained for the binding energy are presented in Secs. III and IV. The definition of the electromagnetic form factors and their relation to single-particle operators is introduced in Sec. V. In Sec. VI the results for the electromagnetic form factors and observables are presented and discussed. Finally, in Sec. VII some conclusions are summarized.

II. TWO-BODY INTERACTIONS

The phenomenological two-body potentials chosen to represent the interaction between particles in each pair, reproduce the low-energy phase shifts, have a simple analytical expression, and are widely used in the literature for different applications.

The n-α potential is represented by a set of momentum-space separable interactions for the dominant partial waves at low energy $(\ell_j)=S_{1/2}$, $P_{1/2}$, and $P_{3/2}$. The potential operator, with one separable term in each partial wave, has the general form

$$V_{n\alpha}=\sum_{\ell j m_j}|f_{\ell j m_j}\rangle\lambda_{\ell j}\langle f_{\ell j m_j}|, \tag{1}$$

in which $\lambda_{\ell j}$ is the interaction strength, and the operational form factor has the following representation in momentum space:

TABLE I. Parameters for the dominant partial-wave interactions in the two-body n-α potential, extracted from Ref. [9].

ℓ_j	Name	$\frac{2\mu_{n\alpha}}{4\pi}\lambda_{\ell j}$ (fm$^{-3-2\ell}$)	$\beta_{\ell j}$ (fm^{-1})
$S_{1/2}$	LRG	0.6373	0.7496
	GL1	0.3	0.7
	GL2	0.2	0.6
$P_{1/2}$	LRG	−1.1040	1.1770
	S	−0.1640	0.8505
$P_{3/2}$	LRG	−4.8310	1.4490
	S	−1.3671	1.1352

$$\langle \boldsymbol{q}|f_{\ell j m_j}\rangle = f_{\ell j}(q)\sum_{ms}\langle \ell m\, \tfrac{1}{2}\, s|jm_j\rangle Y_{\ell m}(\hat{\boldsymbol{q}})\chi_s^{1/2}. \quad (2)$$

In the present work, the functional form factor $f_{\ell j}(q)$ is given analytically by a simple one-parameter expression which leads to the correct threshold and asymptotic behavior of the phase shifts [8]:

$$f_{\ell j}(q) = \frac{q^\ell}{(q^2+\beta_{\ell j}^2)^{\ell+1}}, \quad (3)$$

where $\beta_{\ell j}$ acts as the inverse range of the interaction.

The particular range and strength parameters of these interactions which are of primary interest in the present calculations correspond to the designated ''preferred set'' of Lehman, Rai, and Ghovanlou [9], in their analysis of different n-α interactions. They are listed in Table I under the designation of LRG. This set of interactions reproduces with great accuracy the n-α experimental phase shifts up to about 15 MeV, and was used with great success in the three-body model study of the $A=6$ systems (^{6}He and ^{6}Li) [8,9].

Different parametrizations of the various n-α partial wave interactions were tested in order to estimate the sensitivity of the model to the two-body input. All n-α interactions described in the above references with form factors presenting the proper asymptotic behavior (3) were considered in these tests. In partial wave $S_{1/2}$, interactions GL1 and GL2 represent improvements to the LRG fit but in limited energy regions: GL1 fits the very low-energy phase shifts, while GL2 fits the 10–15 MeV region. Extensively used in the past, the interactions designated by S, from Shanley [10], in both $P_{1/2}$ and $P_{3/2}$ partial waves, produce comparatively poor fits to the phase shifts. The results showed no particular sensitivity of either the binding energy or the electromagnetic observables to the various interactions used in partial waves $S_{1/2}$ and $P_{1/2}$ (the variations in most observables did not exceed 2%). Although not as accurately fitted to the two-body experimental data as the LRG, the interaction S, in the dominant $P_{3/2}$ partial wave, has the advantage of producing a very good result for the ^{9}Be ground-state energy, and thus permitting the observation of the scaling of the electromagnetic properties with the binding energy.

The nuclear interaction between the two alpha particles is represented by the well-known Ali-Bodmer (AB) potential [11]. This is a configuration-space local potential acting in partial waves $\ell=0$, 2, and 4, with the radial dependence represented by the sum of two Gaussian functions. The potential operator has the general form

$$V_{\alpha\alpha} = \sum_{\ell m}\int dr r^2 |r\ell m\rangle V_\ell(r)\langle r\ell m|, \quad (4)$$

with

$$V_\ell^{\rm AB}(r) = V_{r\ell}\exp(-\mu_{r\ell}^2 r^2) + V_{a\ell}\exp(-\mu_{a\ell}^2 r^2). \quad (5)$$

In order to determine the sensitivity of the results to the particular two-body interaction, an alternative α-α potential is also tested: the Chien-Brown (CB) potential [12]. This is also a configuration-space local potential in each partial wave (4), with a distinct analytical form for the attractive term, and acting also in $\ell=6$. In both potentials the attractive term is common to all partial waves.

The use of these potentials in a momentum space calculation like the present one requires their Fourier transformation:

$$V_{\alpha\alpha} = \sum_{\ell m}\int dq q^2 dq' q'^2 |q\ell m\rangle V_\ell(q,q')\langle q'\ell m|, \quad (6)$$

where

$$V_\ell(q,q') = \frac{2}{\pi}\int dr r^2 j_\ell(qr) V_\ell(r) j_\ell(q'r). \quad (7)$$

This Fourier transformation can be performed numerically with great accuracy, however, for the Ali-Bodmer potential one is able to obtain an analytic expression for the potential terms in momentum space:

$$V_\ell^{\rm AB}(q,q') = \sum_{i=r,a}\frac{V_{i\ell}}{2\mu_{i\ell}^2\sqrt{qq'}} \times \exp\left(-\frac{q^2+q'^2}{4\mu_{i\ell}^2}\right) I_{\ell+1/2}\left(\frac{qq'}{2\mu_{i\ell}^2}\right), \quad (8)$$

where $I_{\ell+1/2}(x)$ is the Bessel function of imaginary argument [13].

The Coulomb potential between the alpha particles is represented by its partial wave expansion in momentum space (6), expressed in terms of the Legendre function of the second kind:

$$V_\ell^C(q,q') = Z_\alpha^2 e^2 \frac{1}{\pi qq'} Q_\ell\left(\frac{q^2+q'^2}{2qq'}\right), \quad (9)$$

where $Z_\alpha e$ is the total charge of the alpha particle.

In order to keep the calculation amenable, this expansion is truncated after partial wave $\ell=8$. This option is justified *a posteriori* by the calculation of the contributions to the bound-state Coulomb energy from the various partial waves. It is found that these contributions decrease very rapidly for $\ell>2$, with the $\ell=8$ term representing less than 0.02% of the total.

III. THREE-BODY BOUND-STATE EQUATIONS

The primary purpose of the three-body formulation of the momentum-space $n+\alpha+\alpha$ bound-state equations, with Coulomb interaction between the two alpha particles, is to obtain both the binding energy and the wave function.

The Coulomb interaction between the pair of charged particles is included in the three-body equations using a method that is independent of the form of the nuclear interaction. In this method, presented by Lehman *et al.* [7], the equations for the bound-state wave function components do not involve the Coulomb t matrix, but only the Coulomb potential. A set of two-variable integral equations is obtained after partial wave projection, even with the use of separable two-body nuclear potentials, because of the local character of the Coulomb potential. However, these two-variable equations are easily solved numerically permitting the direct construction of the bound-state wave function.

The method described in Ref. [7] is generalized here in order to include unequal-mass particles and spin degrees of freedom, and also to allow the use of nonseparable nuclear potentials.

Considering particle 1 to be the neutron and designating the alpha particles by 2 and 3, in the present three-body model of ^{9}Be the Hamiltonian is expressed by

$$H=H_0+V_1+V_1^C+V_2+V_3, \tag{10}$$

where H_0 is the free-particle Hamiltonian, V_i denotes the nuclear potential between the particles of pair i, and V_1^C represents the Coulomb potential between the alpha particles. The bound-state wave function Ψ, which is a solution of the eigenvalue equation

$$H\Psi=E\Psi \quad (E<0), \tag{11}$$

is decomposed into the three standard Faddeev components corresponding to the three possible two-cluster partitions of the system

$$\Psi=\Psi_1^C+\Psi_2+\Psi_3. \tag{12}$$

The equations that determine these components are

$$(H_0-E)\Psi_i=-V_i\Psi \quad (i=2,3), \tag{13}$$

$$(H_0-E)\Psi_1^C=-(V_1+V_1^C)\Psi. \tag{14}$$

The component Ψ_1^C, corresponding to partition $(\alpha\alpha)n$, is now further decomposed into a ''Coulomb-modified'' nuclear part Ψ_1, and a ''pure'' Coulomb component Ψ_4, satisfying the equations

$$(H_0-E)\Psi_1=-V_1\Psi, \tag{15}$$

$$(H_0-E)\Psi_4=-V_1^C\Psi. \tag{16}$$

The full bound-state wave function is given now by the sum of four components

$$\Psi=\Psi_1+\Psi_2+\Psi_3+\Psi_4. \tag{17}$$

Each of the equations for the nuclear components can be expressed in terms of the nuclear two-body t matrix for the corresponding pair $T_i(E)$, and the free-particle resolvent $G_0(E)=(E-H_0)^{-1}$. The α-α t matrix embedded in three-body space is a function of the Jacobi momenta of partition 1 (the appropriate to represent the α-α interaction), of the form

$$\langle 1:\boldsymbol{qQ}|T_1(E)|1:\boldsymbol{q}'\boldsymbol{Q}'\rangle=\delta(\boldsymbol{Q}-\boldsymbol{Q}')\sum_{\ell m} Y_{\ell m}(\hat{\boldsymbol{q}})Y^*_{\ell m}(\hat{\boldsymbol{q}}') \times t_\ell\left(E-\frac{Q^2}{2\mu_1};q,q'\right), \tag{18}$$

where the two-body t matrix results from the Lippmann-Schwinger equation:

$$t_\ell(E_{(2)};q,q')=V_\ell(q,q')+\int_0^\infty dq''q''^2\frac{V_\ell(q,q'')}{E_{(2)}-q''^2/2\nu_1} \times t_\ell(E_{(2)};q'',q'). \tag{19}$$

The n-α t matrix is obtained in a separable form

$$\langle 2:\boldsymbol{qQ}|T_2(E)|2:\boldsymbol{q}'\boldsymbol{Q}'\rangle=\delta(\boldsymbol{Q}-\boldsymbol{Q}')\langle\boldsymbol{q}|f_{\ell jm_j}\rangle\tau_{\ell j}\left(E-\frac{Q^2}{2\mu_2}\right) \times\langle f_{\ell jm_j}|\boldsymbol{q}'\rangle, \tag{20}$$

with

$$\tau_{\ell j}(E_{(2)})=\left(\lambda_{\ell j}^{-1}-\int_0^\infty dq''q''^2\frac{|f_{\ell j}(q'')|^2}{E_{(2)}-q''^2/2\nu_2}\right)^{-1}. \tag{21}$$

The two- and three-body reduced masses, appearing in the above equations, are defined as $\nu_i=m_jm_k/M_{jk}$, $\mu_i=m_iM_{jk}/M$, where (i,j,k) represent any permutation of (1,2,3), and with the pair and total masses: $M_{jk}=m_j+m_k$ and $M=m_n+2m_\alpha$.

Hence, the coupled equations that are solved in momentum space for the bound-state wave function components of the system take the form

$$\Psi_i=G_0(E)T_i(E)(\Psi_j+\Psi_k+\Psi_4), \tag{22a}$$

$$\Psi_4=G_0(E)V_1^C(\Psi_1+\Psi_2+\Psi_3+\Psi_4), \tag{22b}$$

with $i,j,k=1,2,3;\ i\neq j\neq k\neq i$.

Notice that in the equation for the Coulomb component Ψ_4, the Coulomb t matrix is not introduced. It is an important feature of this formulation that the equations involve only the Coulomb potential V_1^C between the pair of charged particles and not the Coulomb t matrix. A different approach to the momentum space three-body problem with two charged particles, that includes the Coulomb t matrix in the equations, was described by Kok and van Haeringen [14].

It is convenient to introduce at this point the total angular momentum representation of the Jacobi coordinates. For each partition this representation is made up of all three-body channel states resulting from the partial wave expansion of

the Jacobi momenta coupled with the spin of the neutron to total angular momentum J and projection M_J. The channel states are

$$\mathcal{Y}^{JM_J}_{\ell(1/2)jL}(\hat{\boldsymbol{q}},\hat{\boldsymbol{Q}}) \equiv \langle i{:}\boldsymbol{qQ}|i{:}qQ;(\ell(1/2)jL)JM_J\rangle = \sum_{msm_jM} \langle \ell(1/2)\, ms|jm_j\rangle \times \langle jLm_jM|JM_J\rangle Y_{\ell m}(\hat{\boldsymbol{q}}) Y_{LM}(\hat{\boldsymbol{Q}}) \chi_s^{1/2}.$$

In the present notation ℓ represents the relative orbital angular momentum of the particles that form the pair in the partition considered, j is the channel spin which results from the coupling of ℓ with the spin of the neutron, and L represents the relative orbital angular momentum between the pair and the third particle.

In order to lighten the notation it is usually represented by $\gamma_{(i)}$, the complete set of angular momentum variables $[\ell(1/2)jL]_{(i)}$ that uniquely identifies each channel state for fixed total angular momentum J and projection M_J in a given partition i. If the partition is specified elsewhere the subscript may be omitted. The basis states of this representation $|i{:}qQ;[\ell(1/2)jL]JM_J\rangle$ may be more compactly denoted by $|i{:}qQ;\gamma\rangle$. The four components of the wave function are projected onto the angular momentum representation associated with the corresponding partition. Notice that the partition in which Ψ_4 is projected, called partition 4 for notation consistency, is the same as partition 1. The projected wave function components are denoted by

$$\Psi_{i\gamma}(q,Q) \equiv \langle i{:}qQ;\gamma|\Psi_i\rangle.$$

The characteristics of the wave function with respect to symmetry and parity are easily analyzed in this representation. The wave function must be symmetric upon interchange of the two alpha particles (particles 2 and 3). This interchange transforms partition 2 into partition 3 and vice versa. From the condition of symmetry it follows that the dependence of the wave function on the variables of partitions 2 and 3 is identical: $\langle 3{:}qQ;\gamma|\Psi\rangle = \langle 2{:}qQ;\gamma|\Psi\rangle$. Thus, the equation for Ψ_3 may be eliminated in Eq. (22a) as it is identical to the equation for Ψ_2. In partition 1 the exchange of the two alpha particles corresponds to changing the pair relative momentum $\boldsymbol{q}$ into $-\boldsymbol{q}$. The symmetry of the wave function leads to the condition $\langle 1{:}qQ;\gamma|\Psi\rangle = (-1)^{\ell}\langle 1{:}qQ;\gamma|\Psi\rangle$, from which it is straightforward to conclude that the bound state of the system allows only even relative angular momenta between the alpha particles. Finally, from the conservation of parity $\mathcal{P}$, one obtains the following condition involving the two orbital angular momenta ℓ and L, in every partition: $(-1)^{\ell+L} = \mathcal{P}$.

Introducing the explicit form of the two-body interaction operators T_i and V_1^C, and the appropriate partitions of unity, the equations for the bound-state wave function components (22) become, in the total angular momentum representation,

$$\Psi_{2\gamma}(q,Q) = \frac{1}{E-(Q^2/2\mu_2)-(q^2/2\nu_2)} \times f_{\ell_j}(q)\tau_{\ell_j}(E-Q^2/2\mu_2) \times \int dq'' q''^2 f_{\ell_j}(q'') \sum_{i=1,3,4} \sum_{\gamma'_{(i)}} \times \int dq' q'^2 dQ' Q'^2 \times \langle 2{:}q''Q;\gamma|i{:}q'Q';\gamma'\rangle \Psi_{i\gamma'}(q',Q'), \quad (23a)$$

$$\Psi_{1\gamma}(q,Q) = \frac{1}{E-(Q^2/2\mu_1)-(q^2/2\nu_1)} \times \int dq'' q''^2 t_{\ell}(E-Q^2/2\mu_1;q,q'') \times \sum_{i=2,3,4} \sum_{\gamma'_{(i)}} \int dq' q'^2 dQ' Q'^2 \times \langle 1{:}q''Q;\gamma|i{:}q'Q';\gamma'\rangle \Psi_{i\gamma'}(q',Q'), \quad (23b)$$

$$\Psi_{4\gamma}(q,Q) = \frac{1}{E-(Q^2/2\mu_1)-(q^2/2\nu_1)} \int dq'' q''^2 V^C_{\ell}(q,q'') \times \sum_{i=1,2,3,4} \sum_{\gamma'_{(i)}} \int dq' q'^2 dQ' Q'^2 \times \langle 4{:}q''Q;\gamma|i{:}q'Q';\gamma'\rangle \Psi_{i\gamma'}(q',Q'). \quad (23c)$$

Each sumation index $\gamma'_{(i)} \equiv [\ell'(1/2)j'L']_{(i)}$ represents one channel of partition i included in the equations. The summations are extended to all the channels compatible with the terms of the two-body interactions acting between the particles of the pair in the given partition.

The structure of Eq. (23) points out to the following form of the wave function components:

$$\Psi_{2\gamma}(q,Q) = \frac{1}{E-(Q^2/2\mu_2)-(q^2/2\nu_2)} f_{\ell_j}(q) G_{2\gamma}(Q), \quad (24a)$$

$$\Psi_{i\gamma}(q,Q) = \frac{1}{E-(Q^2/2\mu_1)-(q^2/2\nu_1)} \tilde{\Psi}_{i\gamma}(q,Q) \quad (i=1,4). \quad (24b)$$

For Ψ_2, the component associated with partitions of the type $(n\alpha)\alpha$, the dependence on the two Jacobi momenta is factorized due to the separable nature of the n-α interactions. The spectator function $G_{2\gamma}(Q)$ gives the γ-channel momentum distribution of one of the alpha particles relative to the center of mass of the pair formed by the other alpha particle and the neutron.

The matrix elements that represent the overlap of the channel states of any two partitions have the general form

$$\langle i{:}qQ;\gamma|i'{:}q'Q';\gamma'\rangle=\int d\hat{\boldsymbol{q}}d\hat{\boldsymbol{q}}'d\hat{\boldsymbol{Q}}d\hat{\boldsymbol{Q}}'\mathcal{Y}^{JM_J*}_{\ell(1/2)jL}(\hat{\boldsymbol{q}},\hat{\boldsymbol{Q}})\times\mathcal{Y}^{JM_J}_{\ell'(1/2)j'L'}(\hat{\boldsymbol{q}}',\hat{\boldsymbol{Q}}')\times\langle i{:}\boldsymbol{qQ}|i'{:}\boldsymbol{q}'\boldsymbol{Q}'\rangle, \tag{25}$$

where the matrix elements $\langle i{:}\boldsymbol{qQ}|i'{:}\boldsymbol{q}'\boldsymbol{Q}'\rangle$ are given by Dirac δ functions relating the Jacobi momentum coordinates of the two partitions i and i'.

The situation in which the left and right partitions are the same ($i=i'$) is trivial. For $i\neq i'$ it is convenient to consider two forms of establishing this relation, depending on the momentum variables that are taken as independent:

$$\langle i{:}\boldsymbol{qQ}|i'{:}\boldsymbol{q}'\boldsymbol{Q}'\rangle=\delta(\boldsymbol{q}-\boldsymbol{k}_{ii'}(\boldsymbol{Q},\boldsymbol{Q}'))\delta(\boldsymbol{q}'-\boldsymbol{k}'_{ii'}(\boldsymbol{Q},\boldsymbol{Q}'))=\delta(\boldsymbol{q}'-\overline{\boldsymbol{k}}_{ii'}(\boldsymbol{Q},\boldsymbol{q}))\delta(\boldsymbol{Q}'-\overline{\boldsymbol{K}}_{ii'}(\boldsymbol{Q},\boldsymbol{q})),$$

where $\boldsymbol{k}$, $\boldsymbol{k}'$, $\overline{\boldsymbol{k}}$, and $\overline{\boldsymbol{K}}$ designate certain vector compositions of the Jacobian momenta with coefficients involving the masses of the particles. After introducing either of these two forms in Eq. (25), expanding the arguments of the channel state functions, recoupling the angular momentum coefficients and performing the possible angular integrations, one arrives at the following expressions for the overlap of two channel states:

$$\langle i{:}qQ;\gamma|i'{:}q'Q';\gamma'\rangle=\int_{-1}^{+1}duP^{ii'}_{\gamma\gamma'}(Q,Q',u)\frac{\delta(q-k_{ii'}(Q,Q',u))}{q^2}\frac{\delta(q'-k'_{ii'}(Q,Q',u))}{q'^2}=\int_{-1}^{+1}du\overline{P^{ii'}_{\gamma\gamma'}}(Q,q,u)\frac{\delta(q'-\overline{k}_{ii'}(Q,q,u))}{q'^2}\frac{\delta(Q'-\overline{K}_{ii'}(Q,q,u))}{Q'^2}.$$

The integration variable u represents the cosine of the angle between the directions of the two independent momenta, either $\hat{\boldsymbol{Q}}\cdot\hat{\boldsymbol{Q}}'$ or $\hat{\boldsymbol{Q}}\cdot\hat{\boldsymbol{q}}$. The functional form of the scalar coefficients P and $\overline{P}$ and the magnitude of the composed momenta are presented in the Appendix.

Finally, a set of coupled homogeneous integral equations for the spectator function G_2 and the redefined wave function components $\widetilde{\Psi}_1$ and $\widetilde{\Psi}_4$ are obtained in the form

$$G_{2\gamma}(Q)=\tau_{\ell j}\left(E-\frac{Q^2}{2\mu_2}\right)\int_0^\infty dQ'Q'^2\int_{-1}^{+1}du\left[\frac{f_{\ell j}(k_{22})}{E-(Q'^2/2\mu_2)-(k'^2_{22}/2\nu_2)}\sum_{\gamma'_{(2)}}P^{22}_{\gamma\gamma'}(Q,Q',u)f_{\ell'j'}(k'_{22})G_{2\gamma'}(Q')+\frac{f_{\ell j}(k_{21})}{E-(Q'^2/2\mu_1)-(k'^2_{21}/2\nu_1)}\sum_{i=1,4}\sum_{\gamma'_{(i)}}P^{2i}_{\gamma\gamma'}(Q,Q',u)\widetilde{\Psi}_{i\gamma'}(k'_{21},Q')\right], \tag{26a}$$

$$\widetilde{\Psi}_{1\gamma}(q,Q)=\int_0^\infty dq'q'^2t_{\ell}\left(E-\frac{Q^2}{2\mu_1};q,q'\right)\left[2\int_{-1}^{+1}du\sum_{\gamma'_{(2)}}\overline{P^{12}_{\gamma\gamma'}}(Q,q',u)\frac{f_{\ell'j'}(\overline{k}_{12})}{E-(\overline{K}^2_{12}/2\mu_2)-(\overline{k}^2_{12}/2\nu_2)}G_{2\gamma'}(\overline{K}_{12})+\frac{1}{E-(Q^2/2\mu_1)-(q'^2/2\nu_1)}\sum_{\gamma'_{(4)}}\delta_{\gamma\gamma'}\widetilde{\Psi}_{4\gamma'}(q',Q)\right], \tag{26b}$$

$$\widetilde{\Psi}_{4\gamma}(q,Q)=\int_0^\infty dq'q'^2V^C_{1\gamma}(q,q')\left[2\int_{-1}^{+1}du\sum_{\gamma'_{(2)}}\overline{P^{42}_{\gamma\gamma'}}(Q,q',u)\frac{f_{\ell'j'}(\overline{k}_{12})}{E-(\overline{K}^2_{12}/2\mu_2)-(\overline{k}^2_{12}/2\nu_2)}G_{2\gamma'}(\overline{K}_{12})+\frac{1}{E-(Q^2/2\mu_1)-(q'^2/2\nu_1)}\left(\sum_{\gamma'_{(1)}}\delta_{\gamma\gamma'}\widetilde{\Psi}_{1\gamma'}(q',Q)+\widetilde{\Psi}_{4\gamma}(q',Q)\right)\right]. \tag{26c}$$

TABLE II. Results for the ground-state binding energy, in the three-body model of ^{9}Be, obtained with different two-body interactions.

	α-α	
n-α	AB	CB
LRG	−2.090	−2.156
GL1($S_{1/2}$)	−2.093	−2.165
GL2($S_{1/2}$)	−2.051	−2.114
S($P_{1/2}$)	−2.070	−2.134
S($P_{3/2}$)	−1.530	−1.449
Expt.	−1.5735 [a]	

[a]Reference [17].

The partial wave projection of the Coulomb potential $V^C_{\not\ell}(q,q')$ is responsible for the presence of a logarithmic singularity in the integrand of the last equation. This singularity is handled using a subtraction method introduced by Landé [15,7].

IV. SOLUTION OF THE EQUATIONS

Once the three-body equations are established, one proceeds to its numerical solution. The integrations are performed by introducing Gegenbauer quadratures in the momentum variables Q' and q', and a Legendre quadrature for the integration in variable u. The values of the variables that represent the magnitude of the Jacobi momenta Q and q are set at the same mesh points as the Gegenbauer quadratures. The unknown functions G_2, $\tilde{\Psi}_1$, and $\tilde{\Psi}_4$ on the right-hand side of the equations are interpolated with the use of splines. The set of integral equations then become a system of algebraic equations of the form $AX=X$. This is simply a special case of the matrix eigenvalue problem $AX=\lambda X$, which is solved by the method of inverse iteration, as described in its application to three-body problems by Glöckle [16]. The total energy is varied until an eigenvalue of 1 is found for the matrix equation. The energy thus encountered is the binding energy and the corresponding eigenvector is formed by the bound-state wave function components. From these components one goes back to Eqs. (24) and (17), and obtains the full bound-state wave function. After normalization this wave function is available for future applications.

The ground state of ^{9}Be is characterized by total spin and parity $J^P=(3/2)^-$. The present calculation includes all three-body channels that couple to this total spin and parity, and are compatible with the two-body interactions described in Sec. II. This makes up a total of 30 channels, when the AB potential is used.

The binding energies resulting from different two-body interactions are presented in Table II. It is immediately recognizable that the energies obtained with the AB potential are in all cases closer to the experimental value than those resulting from the CB potential. Remarkably, the same situation was verified with respect to most other observables. On the other hand, the use of the n-α $P_{3/2}$ interaction S results in a binding energy much closer to the experimental value than the LRG. Nevertheless, this situation seems to be accidental, since further tests indicated that the value of the electromagnetic observables obtained with the corresponding wave function are farther away from the experimental values. No significant differences are encountered by changing the n-α $S_{1/2}$ and $P_{1/2}$ interactions.

The bound-state energy of the $n+\alpha+\alpha$ system obtained with the interactions of primary interest is $E_B=-2.090$ MeV. This result is not very close to the experimental value of -1.5735 MeV [17]. However, the binding energy results from the near cancellation of two dynamical terms with opposite sign and very large absolute value: the kinetic and potential energies. This fact explains how a small imprecision in the two-body potential term, like for instance of the order of 2%, is accountable for the large relative difference in the resulting binding energy. In conclusion, the failure to reproduce the correct binding energy is by no means an indication that the dynamics of the system has been missed out or that the wave function is inadequate. The behavior of the wave function and how it reproduces the dynamics of the nuclear state is the most important concern; this may be tested in greater detail through the application of the electromagnetic multipole operators.

V. ELECTROMAGNETIC FORM FACTORS

The experimental elastic electron scattering angular differential cross section is parametrized, in the plane-wave Born approximation, in terms of the longitudinal and transverse form factors, both dependent on the momentum transfer [18,1]:

$$\frac{d\sigma}{d\Omega}=Z^2\sigma_M f_R\{V_L(\theta)|F_L(q)|^2+V_T(\theta)|F_T(q)|^2\}. \quad (27)$$

These form factors represent the effect on the cross section due to the internal structure of the target nucleus. Once the ground-state target nuclear wave function is known, the elastic longitudinal and transverse form factors can be theoretically evaluated.

All nonzero matrix elements of the charge (Coulomb) and magnetic multipole operators

$$F_{C\mathcal{L}}(q)=\frac{1}{Z}\left(\frac{4\pi}{2J+1}\right)^{1/2}\langle\Psi^{(J)}||\hat{M}^C_{\mathcal{L}}(q)||\Psi^{(J)}\rangle, \quad (28)$$

$$F_{M\mathcal{L}}(q)=\frac{1}{Z}\left(\frac{4\pi}{2J+1}\right)^{1/2}\langle\Psi^{(J)}||\hat{M}^M_{\mathcal{L}}(q)||\Psi^{(J)}\rangle, \quad (29)$$

contribute, respectively, to the longitudinal and transverse form factors

$$|F_L(q)|^2=\sum_{\mathcal{L}=0}^{2J}|F_{C\mathcal{L}}(q)|^2 \quad (\mathcal{L}\ \text{even}), \quad (30)$$

$$|F_T(q)|^2=\sum_{\mathcal{L}=1}^{2J}|F_{M\mathcal{L}}(q)|^2 \quad (\mathcal{L}\ \text{odd}). \quad (31)$$

The ^{9}Be ground state, having $J=3/2$, possesses only charge monopole and quadrupole, and magnetic dipole and octupole form factors. The multipole operators are defined in terms of the charge and current density operators in the usual form:

$$\hat{M}^C_{\mathcal{LM}}(q)=\int d\boldsymbol{r} j_{\mathcal{L}}(qr)Y_{\mathcal{LM}}(\hat{\boldsymbol{r}})\hat{\rho}(\boldsymbol{r}), \tag{32}$$

$$\hat{M}^M_{\mathcal{LM}}(q)=\int d\boldsymbol{r} j_{\mathcal{L}}(qr)Y_{\mathcal{LLM}}(\hat{\boldsymbol{r}})\cdot\hat{\boldsymbol{J}}(\boldsymbol{r}). \tag{33}$$

The ^{9}Be nuclear charge and current densities are assumed to be the sum of the charges and currents due to each of the three particles in the system; i.e., the operators $\hat{\rho}$ and $\hat{\boldsymbol{J}}$ are expressed in terms of single-particle operators. The current density can be decomposed into a convection current part and a magnetization part due to the neutron spin [19,20]:

$$\hat{\rho}(\boldsymbol{r})=\sum_{j=n,\alpha,\alpha}\hat{\rho}_j(\boldsymbol{r}-\boldsymbol{r}_j), \tag{34}$$

$$\hat{\boldsymbol{J}}(\boldsymbol{r})=\sum_{j=n,\alpha,\alpha}\frac{\hbar}{m_jc}\frac{1}{2}[\hat{\boldsymbol{p}}_j\hat{\rho}_j(\boldsymbol{r}-\boldsymbol{r}_j)+\hat{\rho}_j(\boldsymbol{r}-\boldsymbol{r}_j)\hat{\boldsymbol{p}}_j] + \frac{\hbar}{2m_nc}\nabla\times\hat{\boldsymbol{\sigma}}_n\hat{\mu}_n(\boldsymbol{r}-\boldsymbol{r}_n). \tag{35}$$

Meson exchange currents are not taken into consideration, but the finite particle sizes are accounted for by introducing phenomenological particle form factors. If the constituents were point particles the corresponding densities would be represented by Dirac delta functions: $\hat{\rho}_j(\boldsymbol{r}-\boldsymbol{r}_j)=Z_j\delta(\boldsymbol{r}-\boldsymbol{r}_j)$, and $\hat{\mu}_n(\boldsymbol{r}-\boldsymbol{r}_n)=\mu_n\delta(\boldsymbol{r}-\boldsymbol{r}_n)$, where Z_j and μ_n are, respectively, the charge number of particle j and the magnetic moment of the neutron in nuclear magnetons. The finite size of the neutron and the alpha particles and their nonelementary nature are described by the Fourier transforms of the corresponding electric and magnetic form factors [19]:

$$\hat{\rho}_n(\boldsymbol{r}-\boldsymbol{r}_n)=\int\frac{d\boldsymbol{q}}{(2\pi)^3}G_E^{(n)}(q^2)\exp[-i\boldsymbol{q}\cdot(\boldsymbol{r}-\boldsymbol{r}_n)], \tag{36}$$

$$\hat{\mu}_n(\boldsymbol{r}-\boldsymbol{r}_n)=\int\frac{d\boldsymbol{q}}{(2\pi)^3}G_M^{(n)}(q^2)\exp[-i\boldsymbol{q}\cdot(\boldsymbol{r}-\boldsymbol{r}_n)], \tag{37}$$

$$\hat{\rho}_\alpha(\boldsymbol{r}-\boldsymbol{r}_\alpha)=Z_\alpha\int\frac{d\boldsymbol{q}}{(2\pi)^3}G_E^{(\alpha)}(q^2)\exp[-i\boldsymbol{q}\cdot(\boldsymbol{r}-\boldsymbol{r}_\alpha)], \tag{38}$$

$$\hat{\mu}_\alpha(\boldsymbol{r}-\boldsymbol{r}_\alpha)=0. \tag{39}$$

Phenomenological expressions for these particle form factors are obtained from the literature. The neutron charge and magnetic form factors are taken from the work of Gari and Krümpelmann [21]. For the alpha particle charge form factor, the simple parametrization of Frosch *et al.* [22] is used. These phenomenological form factors, together with the two-body potentials described in Sec. II, are the only external input used in the present work.

TABLE III. Results obtained with the present three-body model of the ^{9}Be ground state, and generally accepted experimental values for rms charge radius (r_c), electric quadrupole moment (Q), and magnetic dipole (μ) and octupole (μ_3) moments.

	Present results	Expt. values	Ref.
r_c (fm)	2.477	2.52±0.01	[23]
Q (e fm^2)	4.791	5.3±0.3	[17]
μ (μ_N)	−1.151	−1.1778±0.0009	[17]
μ_3 (μ_N fm^2)	6.01	5±1	[2]

VI. RESULTS AND DISCUSSION

After normalization, the three-body wave function is used in the calculation of the ground-state elastic Coulomb and magnetic form factors, and in the estimation of the electromagnetic observables. The latter, namely rms charge radius, electric quadrupole moment, and magnetic dipole and octupole moments are related to the static limit of the former:

$$r_c=-6\frac{dF_{C0}(q)}{d(q^2)}\bigg|_{q=0}, \tag{40}$$

$$Q=6\,Ze\lim_{q\to0}\frac{F_{C2}(q)}{q^2}, \tag{41}$$

$$\mu=\frac{3\,Z}{\sqrt{10}}\lim_{q\to0}\frac{-iF_{M1}(q)}{q}, \tag{42}$$

$$\mu_3=\frac{3\,Z\sqrt{15}}{2}\lim_{q\to0}\frac{-iF_{M3}(q)}{q^3}. \tag{43}$$

The results obtained for these quantities, using the two-body preferred interactions LRG and AB, are presented in Table III. The values generally accepted for the same quantities which result from analysis of different experimental results are also presented for comparison.

These theoretical results are remarkably good having in mind the simplicity of the model used and the fact that it contains no adjustable parameters.

The electric and magnetic observables associated with the lowest multipoles present a very small relative difference to the corresponding experimental values. The magnetic dipole moment differs from the experimental value, which is known to an extraordinary degree of precision, by less than 2.5%. In the case of the charge radius the difference is less than 2%.

For the highest multipole moments the relative difference is not so small but the results are still quite approximate. The value of the electric quadrupole moment is not very far from the limit of the experimental error interval. In what concerns the magnetic octupole it is important to point out that it is very difficult to establish a reliable experimental value, since this depends to a great extent on the process of analyzing the data and also on the data that are being analyzed. The value estimated by different authors has been varying at least by a factor of 2 over the years. The experimental result used for comparison is taken from the thorough analysis of this quan-

TABLE IV. Results for the ground-state electromagnetic observables, in the three-body model of ^{9}Be, obtained with different two-body interactions.

α-α	n-α	r_c (fm)	Q (e fm^2)	μ (μ_N)	μ_3 (μ_N fm^2)
AB	LRG	2.477	4.791	−1.151	6.01
	GL1($S_{1/2}$)	2.476	4.789	−1.156	6.03
	GL2($S_{1/2}$)	2.477	4.817	−1.136	5.88
	$S(P_{1/2})$	2.477	4.865	−1.081	5.97
	$S(P_{3/2})$	2.558	5.103	−1.243	9.73
CB	LRG	2.450	4.612	−1.130	5.74
	GL1($S_{1/2}$)	2.449	4.604	−1.137	5.76
	GL2($S_{1/2}$)	2.450	4.637	−1.116	5.63
	$S(P_{1/2})$	2.450	4.680	−1.059	5.71
	$S(P_{3/2})$	2.559	5.063	−1.254	9.82

tity made by Lapikás *et al.* [2]. The value of $5\pm1\mu_N$ fm^2 results from the analysis of their experimental scattering data together with older data presented by other authors. However, if the same analysis is applied solely to their data the value they obtain is $6\pm2\mu_N$ fm^2. If this, on the one hand, coincides exactly with the present theoretical result, on the other hand it clearly states the difficulty in establishing a rigorous experimental value.

For comparison, the results for the electromagnetic moments obtained with different sets of two-body interactions are presented in Table IV. Like for the binding energy, the CB potential performs generally worse, and the $S_{1/2}$ and $P_{1/2}$ parametrizations of the n-α interaction have limited influence on the value of the observables. The $P_{3/2}$ interaction S, despite the limitations mentioned in Sec. II, gives a better result for the electric quadrupole moment. However, the magnetic moments, particularly the octupole, are not well reproduced. As expected, the size related observables, charge radius and quadrupole moment, show a scaling with the binding energy in the right direction, but the magnetic observables are oversensitive to a shift in this energy.

It is interesting to examine the single-particle contributions to the matrix elements of the charge and magnetic multipole operators, $F_{C\mathcal{L}}(q)$ and $F_{M\mathcal{L}}(q)$. These contributions are associated with the various terms in the charge and current density operators (34) and (35). In the case of the charge multipole matrix elements the only appreciable contribution comes from the term representing the charge density of the alpha particles. As would be expected, the influence of the finite size of the neutron is negligible. The single-particle contributions to the matrix elements of the magnetic dipole and octupole operators are represented in Fig. 1. It is apparent that the dominant contribution to either $F_{M1}(q)$ or $F_{M3}(q)$ comes from the spin of the neutron, through the magnetization term in Eq. (35). The orbital motion of the charged alpha particles also offers an important contribution, especially to the dipole term in which it has, for low q, the opposite sign to the dominant spin part. As expected, the orbital motion of the neutron presents a negligible effect on both multipole matrix elements.

The squared longitudinal and transverse elastic form factors $|F_L|^2$ and $|F_T|^2$ are represented, respectively, in Figs. 2

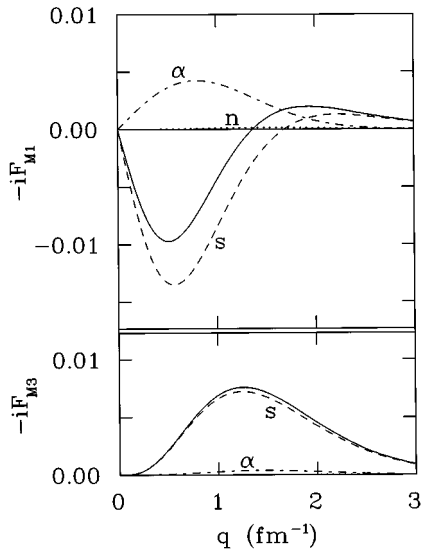

FIG. 1. Single-particle contributions to the matrix elements of the magnetic dipole and octupole operators: neutron spin (s), orbital motion of the alpha particle (α), and orbital motion of the neutron (n).

and 3, as function of the momentum transfer (solid lines). The two Coulomb and two magnetic multipole contributions to these form factors are also represented: the lowest order $|F_{C0}|^2$ and $|F_{M1}|^2$ (dashed lines); and the highest order $|F_{C2}|^2$ and $|F_{M3}|^2$ (dot-dashed lines). The experimental points are taken from some of the most representative elastic electron scattering results for ^{9}Be that span different regions of momentum transfer. These results were published by different authors over the years, since 1966, and culminate in the recent work by Glickman *et al.* [18] where results for

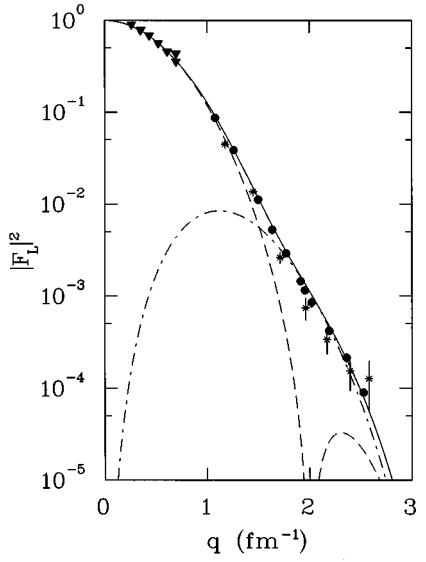

FIG. 2. Squared longitudinal (Coulomb) elastic form factor of ^{9}Be in function of the transfer momentum. The curves represent the present theoretical calculations: total form factor $|F_L|^2$ (solid line), monopole contribution $|F_{C0}|^2$ (dashed line), and quadrupole contribution $|F_{C2}|^2$ (dot-dashed line). The experimental data were extracted from Ref. [18] (circles), Ref. [24] (triangles), and Ref. [3] (stars).

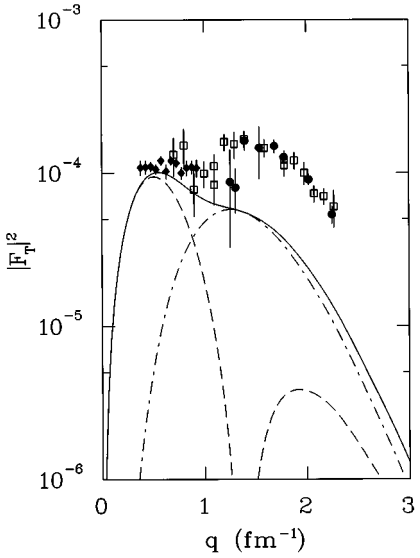

FIG. 3. Squared transverse (magnetic) elastic form factor of ^{9}Be in function of the transfer momentum. The curves represent the present theoretical calculations: total form factor $|F_T|^2$ (solid line), dipole contribution $|F_{M1}|^2$ (dashed line), and octupole contribution $|F_{M3}|^2$ (dot-dashed line). The experimental data were extracted from Ref. [18] (circles), Ref. [2] (diamonds), and Ref. [25] (squares).

both longitudinal and transverse form factors are presented (solid circles).

The calculated longitudinal (Coulomb) form factor describes extremely well the general behavior of the experimental points over the whole region of momentum transfer where data are available. Special mention should be made to the region of the zero of the monopole form factor, where the quadrupole part dominates. The good description also of that region allows the conclusion that the absolute strengths of both quadrupole and monopole terms are very well described by the three-body dynamics of the $n+\alpha+\alpha$ system.

In the case of the transverse form factor, the experimental data are reasonably reproduced in the low-q region. The first maximum of the magnetic dipole term has approximately the right height. However, for higher momentum, the secondary maximum at about 1.9 fm^{-1} is too small in amplitude to reproduce the bump observed in the experimental data points. Also, the analysis of the region where the dipole term has its zero indicates a too small strength of the octupole contribution. This result is extremely interesting, as it indicates that the dynamics of the three-body system, despite reproducing the general trend, is missing something in the description of the high-momentum magnetic scattering properties of ^{9}Be. The same type of discrepancy, between the calculated transverse form factor and the experimental data at large transfer momentum, is found in the case of the three-body $\alpha+p+n$ model of ^{6}Li presented by Eskandarian *et al.* [26]. In fact, these authors obtain for the magnetic dipole term, which constitutes the only contribution to the transverse form factor of ^{6}Li, a reasonable agreement with the experimental data at low q, but their calculation largely underestimates the value of the form factor for higher momenta. These authors attribute part of this discrepancy to the fact that they neglect the convection current contributions, and also to disregarding the Coulomb potential in the dynamical equations of the three-body system. In the present model of ^{9}Be, where both these factors were taken into account, the same kind of disagreement appears, even if not as pronounced. This seems to indicate a common cause, namely the influence of the internal magnetic structure of the alpha particles.

VII. CONCLUSION

The present work constitutes a consistent nonrelativistic three-body calculation of the electromagnetic properties of ^{9}Be. In this formulation of the three-body problem, which allows the inclusion of the Coulomb potential, the bound-state wave function depends exclusively on the low-energy parametrization of the underlying two-body interactions between the constituent particles. Except for the use of phenomenological electromagnetic form factors for the individual particles, which is, of course, necessary in the determination of the electromagnetic properties, no further parametrization is introduced and the results obtained for the physical observables are direct predictions of the three-body model.

This model is very successful in describing the low momentum transfer behavior of the elastic electromagnetic form factors of ^{9}Be. Even beyond its expected domain of validity, for higher values of q, the model is able to reproduce the correct shape of the longitudinal form factor, where both monopole and quadrupole contributions are important. Therefore, the nuclear ground-state charge distribution is entirely compatible with a three-particle structure, where the internal charge distribution of each particle is described by the corresponding charge form factor. The theoretical results obtained for the transverse form factor are physically very interesting because they indicate that, although the model gives a reasonable description of the electron scattering experimental results for low values of momentum transfer, for higher momenta the simple three-body model becomes inadequate. This situation is easily understandable if one has in mind the fact that the greater the penetration of the electrons inside the nucleus, the more the experimental results are going to be sensitive to the details of the internal structure of the alpha particles, and particularly to the distribution of magnetic moments of the nucleons that compose them. The nuclear magnetic moment distribution has to include contributions from configurations other than that of a neutron (with its spin) plus two orbiting charged spinless alpha particles. Many-body correlations play an important role in this case specially at high momentum transfer.

The static properties of the ^{9}Be ground state, which are extracted from the form factors, are predicted with an accuracy comparable and in some cases superior to other theoretical models. The moments of lowest multipolarity, charge radius and magnetic dipole moment, in particular, have their experimental values reproduced within about 2%.

The study of different two-body interactions revealed the importance of having a parametrization of the n-α dominant $P_{3/2}$ partial wave that very well reproduces the low-energy phase shifts. On the other hand, the results demonstrate a large stability with respect to the particular representation of the nondominant partial waves in the n-α system. In the

α-α two-body system, there is not a very marked difference between the use of Ali-Bodmer and Chien-Brown potentials, but it turned out to be the former that produces better results for the static observables as well as for the form factors.

One possible future refinement of the present model might be the attempt to include the nucleonic structure of the alpha particles in the wave function of the system, after the solution of the basic three-body problem. This procedure would perhaps correct the discrepancies found in the transverse form factor at high momentum transfer, by introducing the spin correlations that would affect the matrix elements of the magnetic multipole operators, without destroying the underlying three-body structure of the system.

ACKNOWLEDGMENTS

The author wishes to thank A. C. Fonseca for the suggestion of the present work and also for many fruitful discussions. The author is also thankful to D. R. Lehman for providing helpful information. This research was supported in part by JNICT Grant No. STRDA/C/FIS/1004/93.

APPENDIX: COEFICIENTS INVOLVED IN THE THREE-BODY EQUATIONS

The magnitude of the composed momenta appearing in the final three-body equations (26) have the following definitions:

$$k_{22}(Q,Q',u)=\left|\frac{m_\alpha}{M_{n\alpha}}\boldsymbol{Q}+\boldsymbol{Q}'\right|, \tag{A1}$$

$$k'_{22}(Q,Q',u)=\left|\boldsymbol{Q}+\frac{m_\alpha}{M_{n\alpha}}\boldsymbol{Q}'\right|, \tag{A2}$$

$$k_{21}(Q,Q',u)=\left|\frac{m_n}{M_{n\alpha}}\boldsymbol{Q}+\boldsymbol{Q}'\right|, \tag{A3}$$

$$k'_{21}(Q,Q',u)=\left|\boldsymbol{Q}+\tfrac{1}{2}\boldsymbol{Q}'\right|, \tag{A4}$$

$$\overline{k_{12}}(Q,q',u)=\left|\frac{M}{2M_{n\alpha}}\boldsymbol{Q}+\frac{m_n}{M_{n\alpha}}\boldsymbol{q}'\right|, \tag{A5}$$

$$\overline{K_{12}}(Q,q',u)=\left|\tfrac{1}{2}\boldsymbol{Q}+\boldsymbol{q}'\right|, \tag{A6}$$

where variable u represents either $\hat{\boldsymbol{Q}}\cdot\hat{\boldsymbol{Q}}'$ or $\hat{\boldsymbol{Q}}\cdot\hat{\boldsymbol{q}}'$.

The channel state projection coeficients $P^{ii'}$ and $\overline{P^{ii'}}$ that result from the overlap of channel states in different partitions, are given by the following expressions:

$$P^{22}_{\gamma\gamma'}(Q,Q',u)=\sum_{\lambda=0}^{\ell}\sum_{\lambda'=0}^{\ell'}\sum_{\Lambda=0}^{\Lambda_{\max}}\Theta^{22}_{\gamma\gamma'\lambda\lambda'\Lambda}(-1)^{\ell+\ell'}\left(\frac{m_\alpha}{M_{n\alpha}}\right)^{\ell-\lambda+\lambda'}\left(\frac{Q}{k_{22}}\right)^{\ell}\left(\frac{Q}{k'_{22}}\right)^{\ell'}\left(\frac{Q'}{Q}\right)^{\lambda+\lambda'}\frac{1}{2}P_\Lambda(u), \tag{A7}$$

$$P^{2i}_{\gamma\gamma'}(Q,Q',u)=\sum_{\lambda=0}^{\ell}\sum_{\lambda'=0}^{\ell'}\sum_{\Lambda=0}^{\Lambda_{\max}}\Theta^{2i}_{\gamma\gamma'\lambda\lambda'\Lambda}(-1)^{\ell'}\left(\frac{1}{2}\right)^{\lambda'}\left(\frac{m_n}{M_{n\alpha}}\right)^{\ell-\lambda}\left(\frac{Q}{k_{21}}\right)^{\ell}\left(\frac{Q}{k'_{21}}\right)^{\ell'}\left(\frac{Q'}{Q}\right)^{\lambda+\lambda'}\frac{1}{2}P_\Lambda(u), \tag{A8}$$

$$\overline{P^{i2}_{\gamma\gamma'}}(Q,q',u)=\sum_{\lambda'=0}^{\ell'}\sum_{\lambda''=0}^{L'}-\sum_{\Lambda=0}^{\max}\overline{\Theta^{i2}_{\gamma\gamma'\lambda'\lambda''\Lambda}}(-1)^{L'+\lambda'}\left(\frac{m_n}{M}\right)^{\lambda'}\left(\frac{MQ}{2M_{n\alpha}\overline{k_{12}}}\right)^{\ell'}\left(\frac{Q}{2\overline{K_{12}}}\right)^{L'}\left(\frac{2q'}{Q}\right)^{\lambda'+\lambda''}\frac{1}{2}P_\Lambda(u), \tag{A9}$$

where $P_\Lambda(u)$ is the Legendre polynomial of degree Λ. The limits of the summations in Λ in the above expressions are $\Lambda_{\max}=\min(L'+\lambda+\lambda',L+\ell-\lambda+\ell'-\lambda')$, and $\overline{\Lambda}_{\max}=\min(\ell+\lambda'+\lambda'',L+\ell'-\lambda'+L'-\lambda'')$. The angular momentum coupling coeficients Θ and $\overline{\Theta}$ have the definitions

$$\Theta^{ii'}_{\gamma\gamma'\lambda\lambda'\Lambda}=(-1)^{\ell+\ell'-j-j'-1}\hat{\ell}\hat{\ell}'\hat{j}\hat{j}'\hat{L}\hat{L}'(\hat{\ell-\lambda})(\hat{\ell'-\lambda'})\hat{\Lambda}^2\begin{pmatrix}2\ell+1\\2\lambda\end{pmatrix}^{1/2}\begin{pmatrix}2\ell'+1\\2\lambda'\end{pmatrix}^{1/2}$$
$$\times\sum_{\Lambda'}\hat{\Lambda}'^2\begin{pmatrix}L'&\lambda'&\Lambda'\\0&0&0\end{pmatrix}\begin{pmatrix}\Lambda'&\lambda&\Lambda\\0&0&0\end{pmatrix}\sum_{ABC}\hat{A}^2\hat{B}^2\hat{C}^2\begin{pmatrix}\ell-\lambda&C&L\\0&0&0\end{pmatrix}\begin{pmatrix}C&\ell'-\lambda'&\Lambda\\0&0&0\end{pmatrix}\begin{Bmatrix}L&A&\ell'\\j&\ell&\frac{1}{2}\end{Bmatrix}\begin{Bmatrix}L&A&\ell'\\J&L'&j'\end{Bmatrix}$$
$$\times\begin{Bmatrix}L&B&\Lambda'\\A&\ell&L'\\\ell'&\ell'-\lambda'&\lambda'\end{Bmatrix}\begin{Bmatrix}L&C&\ell-\lambda\\\Lambda'&\Lambda&\lambda\\B&\ell'-\lambda'&\ell\end{Bmatrix}, \tag{A10}$$

$$\overline{\Theta^{ii'}_{\gamma\gamma'\lambda'\lambda''\Lambda}} = (-1)^{\ell+\lambda'+j+j'-1}\hat{\ell}\hat{\ell}'\hat{j}\hat{j}'\hat{L}\hat{L}'(\ell'\hat{-}\lambda')(L'\hat{-}\lambda'')\hat{\Lambda}^2\begin{pmatrix}2\ell'+1\\2\lambda'\end{pmatrix}^{1/2}\begin{pmatrix}2L'+1\\2\lambda''\end{pmatrix}^{1/2}$$
$$\times\sum_{\Lambda'}\hat{\Lambda}'^2\begin{pmatrix}\lambda'' & \lambda' & \Lambda'\\ 0 & 0 & 0\end{pmatrix}\begin{pmatrix}\Lambda' & \ell & \Lambda\\ 0 & 0 & 0\end{pmatrix}\sum_{AB}\hat{A}^2\hat{B}^2\begin{pmatrix}\Lambda & B & L'-\lambda''\\ 0 & 0 & 0\end{pmatrix}\begin{pmatrix}L & B & \ell'-\lambda'\\ 0 & 0 & 0\end{pmatrix}\begin{Bmatrix}L & A & \ell'\\ j & \ell & \frac{1}{2}\\ J & L' & j'\end{Bmatrix}$$
$$\times\begin{Bmatrix}B & \Lambda & L'-\lambda''\\ \lambda' & \Lambda' & \lambda''\\ A & \ell & L'\end{Bmatrix}\begin{Bmatrix}\lambda' & \ell' & \ell'-\lambda'\\ L & B & A\end{Bmatrix}, \tag{A11}$$

where $\hat{x}=\sqrt{2x+1}$, and the summations are extended to all possible values compatible with the triangular conditions imposed by the Wigner symbols.

[1] T. W. Donnelly and I. Sick, Rev. Mod. Phys. **56**, 461 (1984).
[2] L. Lapikás, G. Box, and H. de Vries, Nucl. Phys. **A253**, 324 (1975).
[3] M. Bernheim, T. Stovall, and D. Vinciguerra, Nucl. Phys. **A97**, 488 (1967).
[4] A. C. Fonseca and M. T. Peña, Nucl. Phys. **A487**, 92 (1988).
[5] V. T. Voronchev, V. I. Kukulin, V. N. Pomerantsev, and G. G. Ryzhikh, Few-Body Syst. **18**, 191 (1995).
[6] W. Glöckle, *The Quantum Mechanical Few-Body Problem* (Springer-Verlag, Berlin, 1983).
[7] D. R. Lehman, A. Eskandarian, B. F. Gibson, and L. C. Maximon, Phys. Rev. C **29**, 1450 (1984).
[8] A. Ghovanlou and D. R. Lehman, Phys. Rev. C **9**, 1730 (1974).
[9] D. R. Lehman, M. Rai, and A. Ghovanlou, Phys. Rev. C **17**, 744 (1978).
[10] P. E. Shanley, Phys. Rev. **187**, 1328 (1969).
[11] S. Ali and A. R. Bodmer, Nucl. Phys. **80**, 99 (1966).
[12] W. S. Chien and R. E. Brown, Phys. Rev. C **10**, 1767 (1974).
[13] I. Gradshteyn and I. Ryzhik, *Table of Integrals Series and Products*, 4th ed. (Academic Press, San Diego, 1980).
[14] L. P. Kok and H. van Haeringen, Czech. J. Phys. B **32**, 311 (1982).
[15] Y. R. Kwon and F. Tabakin, Phys. Rev. C **18**, 932 (1978).
[16] W. Glöckle, in *Proceedings of the 8th Autumn School*, Lisboa, 1986, edited by L. S. Ferreira, A. C. Fonseca, and L. Streit, Lecture Notes in Physics Vol. 273 (Springer-Verlag, Berlin, 1987).
[17] F. Ajzenberg-Selove, Nucl. Phys. **A490**, 1 (1988).
[18] J. P. Glickman, W. Bertozzi, T. N. Buti, S. Dixit, F. W. Hersman, C. E. Hyde-Wright, M. V. Hynes, R. W. Lourie, B. E. Norum, J. J. Kelly, B. L. Berman, and D. J. Millener, Phys. Rev. C **43**, 1740 (1991).
[19] A. I. Akhiezer, A. G. Sitenko, and V. K. Tartakovskii, *Nuclear Electrodynamics* (Springer-Verlag, Berlin, 1994).
[20] T. W. Donnelly and J. D. Walecka, Nucl. Phys. **A201**, 81 (1973).
[21] M. F. Gari and W. Krümpelmann, Phys. Lett. **173B**, 10 (1986).
[22] R. F. Frosch, J. S. McCarthy, R. E. Rand, and M. R. Yearian, Phys. Rev. **160**, 874 (1967).
[23] I. Tanihata, H. Hamagaki, O. Hashimoto, Y. Shida, N. Yoshikawa, K. Sugimoto, O. Yamakawa, T. Kobayashi, and N. Takahashi, Phys. Rev. Lett. **55**, 2676 (1985).
[24] J. A. Jansen, R. Peerdeman, and C. de Vries, Nucl. Phys. **A188**, 337 (1972).
[25] R. E. Rand, R. Frosch, and M. R. Yearian, Phys. Rev. **144**, 859 (1966).
[26] A. Eskandarian, D. R. Lehman, and W. C. Parke, Phys. Rev. C **38**, 2341 (1988).